Available online at www.sciencedirect.com

ScienceDirect

IFAC Papers Online CONFERENCE PAPER ARCHIVE

IFAC-PapersOnLine 48-23 (2015) 172–177

Predictive Control with Parameter Adaptation to Achieve α-Protection in the RECONFIGURE Benchmark in the Presence of Icing

E. N. Hartley *

* *University of Cambridge, Department of Engineering, Cambridge, CB2 1PZ. United Kingdom. (e-mail: enh20@eng.cam.ac.uk).*

Abstract: Undetected ice accretions on aerodynamic surfaces can deeply change the dynamic behaviour of aircraft, leading to poor performance of the automatic control systems. This is characterised by oscillatory behaviour, and overshoot of setpoints and flight envelope protection values. To mitigate this undesirable behaviour, this paper applies predictive control in combination with online estimation of the first and second order partial derivatives of the lift and pitching moment coefficients with respect to the angle of attack using an Extended Kalman Filter, to achieve a constrained indirect adaptive flight control law. The design is evaluated on the RECONFIGURE benchmark, which is a nonlinear, high fidelity, industrially validated simulator of a large Airbus aircraft. In icing scenarios at high incidence, the resulting trajectories are shown to be better damped and more compliant with constraints when compared to a predictive control law employing only linear disturbance estimation.

Keywords: Predictive control, Aerospace, Fault Tolerance, Icing, Parameter Estimation

1. INTRODUCTION

Modern civil airliners employ feedback control systems to improve stability, performance and handling characteristics during flight (Favre, 1994; Brière et al., 1995). Since the aircraft dynamics are nonlinear, and the local linearisations vary widely over the flight envelope, to maintain a homogeneous response over the full operating domain, it is typical to schedule linear feedback gains as a function of variables such as airspeed, Mach number, altitude and flap/slat configuration. Protections against exceeding safe angle of attack (AoA), pitch angle and airspeed are also implemented based on measurements of the respective variables. A relatively simple way to accommodate these constraints is with a thresholding and voting approach (e.g., Well (2006)), which modifies the command signal given to an inner loop. An evaluation of various protection schemes can be found in Falkena et al. (2011), and moreover, studies (e.g., Kale and Chipperfield (2004); Keviczky and Balas (2006); Gros et al. (2012)) have shown that constrained model predictive control (MPC) could also be a suitable strategy for this type of application.

The RECONFIGURE project is tasked with investigating and developing advanced aircraft GNC technologies that can improve automated handling of off-nominal events (Goupil et al., 2014) in order to improve performance and reduce pilot workload. One scenario under consideration is undetected ice accretions, which deeply modify the aerodynamic coefficients (Lynch and Khodadoust, 2001; Cebeci and Kafyeke, 2003; Cao et al., 2015). The lift and torque delivered are related to the angle of attack. In normal operation, an increase in angle of attack should increase lift, but once the angle of attack becomes too high for the given flight point a stall will occur and any further increase in angle-of-attack will cause a sharp decrease in lift. Ice accretion can shift this nonlinearity into what should normally be a benign region of operation. This is explained conceptually in Figure 1 for the lift coefficient. Similar effects occur also for the pitching moment and drag coefficients (although drag is not considered in this paper).

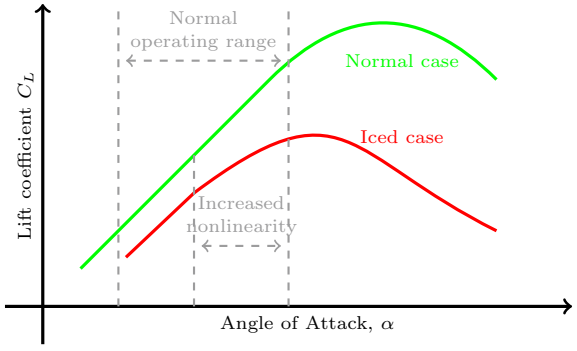

Fig. 1. Qualitative effect ice accretions on lift coefficient (not to scale)

In the benchmark scenarios, the ν-gap (Vinnicombe, 1999) between the linearisations of the short-period models about straight-and-level flight trim points for the nominal and iced cases can be quite small (< 0.1). However, away from the trim point, at high incidence angles, changes in aerodynamic behaviour occur, leading to oscillatory

[1] The research leading to these results has received funding from the European Union Seventh Framework Programme FP7/2007-2013 under grant agreement number 314 544, project "RECONFIGURE".

10.1016/j.ifacol.2015.11.279

behaviour and overshoot of nominal protection values. Detection of icing, and adaptation of flight control laws to also accommodate other off-nominal conditions such as actuator faults has also been an active topic of research. Melody et al. (2000) uses $\mathcal{H}_\infty$ filtering for parameter identification to detect and characterise aircraft icing. In Bragg et al. (2002) a smart anti-icing system based on neural networks is proposed. In Hossain et al. (2003), a relationship is developed offline between the difference in the lift coefficient estimated online and an *a priori* model at low incidence, and the maximum achievable lift. A further linear relationship is used to estimate the maximum acceptable AoA. Sharma et al. (2004) investigates autopilot stability using a PID control, and proposes an adaptive flight envelope protection scheme based on on adaptive stall angle calculation and command limitation. In Tang et al. (2009), a framework for on-line flight envelope estimation is proposed under a general set of faults. In Lombaerts et al. (2009), on-line parameter identification is proposed to identify aerodynamic coefficients in real time, and used to perform nonlinear dynamic inversion to achieve an adaptive fault tolerant controller. In Yu et al. (2014), a "retrospective cost model" refinement technique was applied to estimate deviations in aircraft stability derivatives from their nominal values and identify fault signatures corresponding to icing.

The technological contribution of the present paper is to demonstrate the effectiveness of MPC with parameter adaptation achieved through on-line estimation in handling the scenario of undetected icing in the RECONFIGURE benchmark. The RECONFIGURE benchmark is comprised of a high fidelity, industrially validated, black box nonlinear simulator of a large Airbus aircraft, along with a set of linearisations at representative flight points (Goupil et al., 2014). In the scenarios considered, the trim angle of attack does not substantially change, so it cannot be used as a proxy for the level of icing. Instead, the variation of the aerodynamic coefficients with respect to angle of attack is re-identified in real-time, and these are used to adapt the MPC control law to improve practical performance. Unusually, we use estimates of both the first and second order partial derivatives of the lift and moment coefficients with respect to angle of attack. The latter parameter allows us to anticipate the variation in the linearisation with respect to the angle of attack and is part of the key to the observed improvement in performance.

2. PLANT AND DISTURBANCE MODELS

This study designs an inner loop load-factor control law to provide effective tracking of pilot commands, and angle-of-attack protection under both nominal conditions and conditions where ice accretions have formed, severely modifying the dynamic behaviour. The full nonlinear model is a black box, and therefore the complete aerodynamic model cannot be used for controller design. Instead the first step of our controller design is to construct a quasi-linear-parameter-varying surrogate model based on the provided set of linearisations and standard relationships for the rigid body longitudinal behaviour.

2.1 Construction of internal surrogate model

Airbus has provided the RECONFIGURE consortium with 214 linearisations of the longitudinal dynamics of the nonlinear aircraft model in straight and level flight, over a range of operating conditions. The longitudinal dynamics are traditionally separated into "short period" (high frequency) and "phugoid" (low frequency) modes. Since we wish to control the short-period dynamics, it is normal to treat the phugoid mode as a disturbance. Let m be the mass, I_{yy} be the moment of inertia, q be the pitch rate, α be the angle of attack, V_{TAS} be the true airspeed, n_{za} be the vertical load factor in the aerodynamic frame, n_{zb} be the vertical load factor in the body frame, u_e be the elevator position (assuming all are operating in common mode), u_t be the trimmable horizontal stabiliser (THS) position, and $\delta\bullet$ denote the deviation of variable $\bullet$ from the operating point at which the linearisation was taken, which is in turn indicated with subscript $\bullet_0$. Let c_α be shorthand for $\cos\alpha$. The basic rigid body short-period mode equations at constant speed are

$$\dot{q} = (\overline{q}Sc/I_{yy})C_M \qquad \dot{\alpha} = q - 180n_{za}g/(\pi V_{\mathrm{TAS}})$$
$$n_{za} = (\overline{q}SC_L)/(mg) - \cos\gamma \quad n_{zb} = n_{za}c_\alpha + k_b\dot{q}$$

where S is the wing area, c is the wing chord, $\overline{q} = 0.5\rho V_{\mathrm{TAS}}^2$ is the dynamic pressure, ρ is air density, $g = 9.81\ \mathrm{ms}^{-2}$ is acceleration due to gravity and k_b is a value reflecting the lever arm effect stemming from the load factor sensor (i.e., accelerometer) not being located at the centre of gravity. S and c are fixed for a given aircraft, and $I_{yy} = mk_y^2$, where k_y is the radius of gyration. C_M and C_L are aerodynamic moment and lift coefficients which vary nonlinearly with the flight parameters. For the remainder of this paper we will consider "lumped" values, which include the constant parameters: $\hat{C}_M = Sck_y^2C_M$ and $\hat{C}_L = SC_L$.

At a given flight point, a first-order Taylor approximation of these lumped coefficients can be expressed in the form:

$$\hat{C}_M = \hat{C}_{M0} + \hat{C}_{M_q}\delta q + \hat{C}_{M_\alpha}\delta\alpha + \hat{C}_{M_e}\delta u_e + \hat{C}_{M_t}\delta u_t$$
$$\hat{C}_L = \hat{C}_{L0} + \hat{C}_{L_q}\delta q + \hat{C}_{L_\alpha}\delta\alpha + \hat{C}_{L_e}\delta u_e + \hat{C}_{L_t}\delta u_t.$$

Noting that in straight and level flight, the flight path angle $\gamma = 0$, we can consider a symbolic linearisation of the nonlinear rigid body dynamics about the trim points:

$$\begin{bmatrix}\delta\dot{q}\\ \delta\dot{\alpha}\end{bmatrix} = \begin{bmatrix} k_q\hat{C}_{M_q} & k_q\hat{C}_{M_\alpha}\\ 1 - k_\alpha k_z\hat{C}_{L_\alpha} & -k_\alpha k_z\hat{C}_{L_\alpha}\end{bmatrix}\begin{bmatrix}\delta q\\ \delta\alpha\end{bmatrix} + \begin{bmatrix} k_q\hat{C}_{M_e} & k_q\hat{C}_{M_t}\\ -k_\alpha k_z\hat{C}_{L_e} & -k_\alpha k_z\hat{C}_{L_t}\end{bmatrix}\begin{bmatrix}\delta u_e\\ \delta u_t\end{bmatrix}. \quad (2a)$$

The measured outputs are then

$$q = \delta q + q_0, \quad \alpha = \delta\alpha + \alpha_0 \quad (2b)$$
$$n_{zb} = (k_z\hat{C}_{L_q} + k_z\hat{C}_{L_\alpha})c_{\alpha_0} + k_z\hat{C}_{L_e} + k_z\hat{C}_{L_t} + k_b\dot{q} \quad (2c)$$

where $k_q = \overline{q}/m$, $k_z = \overline{q}/(mg)$, $k_\alpha = 180g/(\pi V_{\mathrm{TAS}})$.

To obtain a continuous model over the flight envelope for these coefficients, we perform a regression of the 214 linearised models against polynomial functions of the flight point data. We first find α_0 and u_{t0} in terms of Mach (M), true airspeed (V_{TAS}), mass (m) and centre of gravity (x_g). We then find polynomial expressions approximating the remaining coefficients. There is a trade-off between the quality of fit and the plausibility of the extrapolation outside of the known points. We therefore

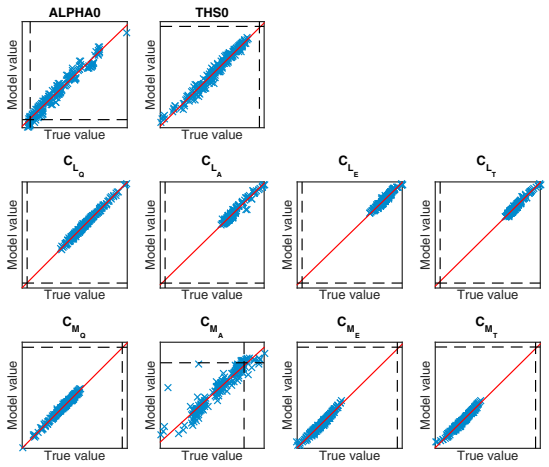

Fig. 2. Regression Quality for Polynomial Surrogate Model

choose a maximum relative order of unity (e.g. relative order 1 in fictitious variables x and y implies an expression of the form $a_0+a_1x+a_2y+a_3xy$). The normalised regression is presented in Figure 2 (zero is marked with dashed lines). The two outliers in $\hat{C}_{M_\alpha}$ correspond to two points at high altitude and high speed, and are not relevant to the scenario being considered here, which affects low altitude and low speed flight points.

2.2 Discretisation and re-arrangement

The polynomial model of the coefficients is used to schedule a linear model of the form (2) over the flight envelope. This is re-arranged and discretised using a zero order hold at a rate $T_s = 0.04$ s, to obtain a discrete time model.

$$\begin{bmatrix} q(k+1) \\ \alpha(k+1) \end{bmatrix} = \underbrace{\begin{bmatrix} \overline{a}_1 & \overline{a}_3 \\ \overline{a}_2 & \overline{a}_4 \end{bmatrix}}_{\overline{A}_{sp}} \underbrace{\begin{bmatrix} q(k) \\ \alpha(k) \end{bmatrix}}_{x_{sp}} + \underbrace{\begin{bmatrix} \overline{b}_1 & \overline{b}_3 \\ \overline{b}_2 & \overline{b}_4 \end{bmatrix}}_{\overline{B}_{sp}} \underbrace{\begin{bmatrix} u_e(k) \\ u_t(k) \end{bmatrix}}_{u_{sp}} + \underbrace{\begin{bmatrix} \overline{e}_1 \\ \overline{e}_2 \end{bmatrix}}_{\overline{e}_{sp}}$$

$$\begin{bmatrix} q(k) \\ \alpha(k) \\ n_{zb}(k) \end{bmatrix} = \underbrace{\begin{bmatrix} 1 & 0 \\ 0 & 1 \\ \overline{c}_1 & \overline{c}_2 \end{bmatrix}}_{\overline{C}_{sp}} \begin{bmatrix} q(k) \\ \alpha(k) \end{bmatrix} + \underbrace{\begin{bmatrix} 0 & 0 \\ 0 & 0 \\ \overline{d}_1 & \overline{d}_2 \end{bmatrix}}_{\overline{D}_{sp}} \begin{bmatrix} u_e(k) \\ u_t(k) \end{bmatrix} + \underbrace{\begin{bmatrix} 0 \\ 0 \\ \overline{f}_1 \end{bmatrix}}_{\overline{f}_{sp}}$$

The affine terms are computed on the basis that the trim points are equilibria as

$$\overline{e}_{sp} = -\overline{A}_{sp}x_{sp,0} - \overline{B}_{sp}u_{sp,0} \quad \overline{f}_{sp} = -\overline{C}_{sp}x_{sp,0} - \overline{D}_{sp}u_{sp,0}.$$

2.3 Disturbance augmentation

The system is augmented with a disturbance model whose states can be estimated (Muske and Badgwell, 2002; Pannocchia and Rawlings, 2003; Maeder et al., 2009). We denote these as

$$w = \begin{bmatrix} \Delta\hat{C}_{M_{\alpha 1}} & \Delta\hat{C}_{M_{\alpha 2}} & \Delta\hat{C}_{L_{\alpha 1}} & \Delta\hat{C}_{L_{\alpha 2}} & w_1 & w_2 & w_3 \end{bmatrix}^T.$$

The first four represent a model of perturbations to the aerodynamic parameters and enter into the system non-linearly. Let $\Delta\hat{C}_{M_\alpha} = (\Delta\hat{C}_{M_{\alpha 1}} + \Delta\hat{C}_{M_{\alpha 2}}(\alpha(k) - \alpha_0))$ and $\Delta\hat{C}_{L_\alpha} = (\Delta\hat{C}_{L_{\alpha 1}} + \Delta\hat{C}_{L_{\alpha 2}}(\alpha(k) - \alpha_0))$.

$$\begin{aligned} q(k+1) = {} & \overline{a}_1 q(k) + (\overline{a}_3 + k_q T_s \Delta\hat{C}_{M_\alpha})\alpha(k) + \overline{b}_1 u_e(k) \\ & + \overline{b}_3 u_t(k) + k_{qw1} w_1(k) + (\overline{e}_1 - k_q T_s \Delta\hat{C}_{M_\alpha}\alpha_0) \quad (5a) \end{aligned}$$

$$\begin{aligned} \alpha(k+1) = {} & \overline{a}_2 q(k) + \left[\overline{a}_4 - k_\alpha k_z T_s \Delta\hat{C}_{L_\alpha}\right]\alpha(k) + \overline{b}_2 u_e(k) \\ & + \overline{b}_4 u_t(k) + k_{\alpha w2} w_2(k) + \overline{e}_2 + k_\alpha k_z T_s \Delta\hat{C}_{L_\alpha}\alpha_0 \quad (5b) \end{aligned}$$

In addition, the load factor in the body axes is

$$\begin{aligned} n_{nb}(k) = {} & \overline{c}_1 q(k) + \left[\overline{c}_2 + k_z c_\alpha \Delta\hat{C}_{L_\alpha} + k_b \Delta\hat{C}_{M_\alpha}\right]\alpha(k) \\ & + \overline{d}_1 u_e(k) + \overline{d}_2 u_t(k) + \overline{f}_1 - \left[k_z c_{\alpha 0} \Delta\hat{C}_{L_\alpha} + k_b \Delta\hat{C}_{M_\alpha}\right]\alpha_0 \\ & + k_b k_{qw1} w_1(k) + k_{zw2} w_2(k) + k_{zw3} w_3(k) \quad (5c) \end{aligned}$$

where $k_{qw1} = T_s/m$, $k_{\alpha w2} = T_s/m$, $k_{zw2} = c_{\alpha 0}/m$, $k_{zw3} = 1/m$. The three additive disturbances representing a scaled pitch rate disturbance, a scaled n_{za} disturbance and an additive disturbance on measurement of n_{zb} are modelled with integrating dynamics, whilst the four parameter estimates are modelled with a decay factor $\tau_d \in [0, 1)$.

$$\begin{aligned} \Delta\hat{C}_{M_{\alpha 1}}(k+1) &= \tau_d \Delta\hat{C}_{M_{\alpha 1}}(k) & w_1(k+1) &= w_1(k) \\ \Delta\hat{C}_{M_{\alpha 2}}(k+1) &= \tau_d \Delta\hat{C}_{M_{\alpha 2}}(k) & w_2(k+1) &= w_2(k) \\ \Delta\hat{C}_{L_{\alpha 1}}(k+1) &= \tau_d \Delta\hat{C}_{L_{\alpha 1}}(k) & w_3(k+1) &= w_3(k) \\ \Delta\hat{C}_{L_{\alpha 2}}(k+1) &= \tau_d \Delta\hat{C}_{L_{\alpha 2}}(k). \end{aligned}$$

System excitation is required to estimate the parameter perturbations, however unexciting, straight and level cruise comprises the majority of commercial journeys. The decay ensures estimations at one point are "forgotten" over time to prevent the erroneous use of data estimated at one flight point at a later time once it has become irrelevant. We set $\tau_d = 0.998$ so that a step change in the estimate remains above 75% of its initial value for approximately 6 s.

2.4 Actuator and sensor dynamics approximation

We model the sensors and elevators as first order lags with time constant 0.1 s, discretised with a zero order hold, with an extra unit delay added to the elevator. In this study we consider the THS position as a measured input disturbance and retain the the default benchmark control law, which moves it as a function of the elevator command. (In the simulation scenarios considered it in fact does not move.) The combined model without disturbances now takes the form

$$\begin{bmatrix} x_f(k+1) \\ x_{sp}(k+1) \\ x_a(k+1) \end{bmatrix} = \underbrace{\begin{bmatrix} A_f & B_f\hat{C}_{sp} & B_f\hat{D}_{spe}C_a \\ & \hat{A}_{sp} & \hat{B}_{spe}C_a \\ & & A_a \end{bmatrix}}_{A_{aug}} \underbrace{\begin{bmatrix} x_f(k) \\ x_{sp}(k) \\ x_a(k) \end{bmatrix}}_{x_{aug}}$$

$$+ \underbrace{\begin{bmatrix} 0 \\ 0 \\ B_a \end{bmatrix}}_{B_{aug}} u_e(k) + \underbrace{\left(\begin{bmatrix} B_f\hat{f}_{sp} \\ \hat{e}_{sp} \\ 0 \end{bmatrix} + \begin{bmatrix} \hat{C}_{sp}\hat{D}_{spt} \\ \hat{B}_{spt} \\ 0 \end{bmatrix} u_t(k)\right)}_{e_{aug}}$$

$$y_{out}(k) = \underbrace{[C_f \ 0 \ 0]}_{C_{aug}} x_{aug},$$

where $(A_f, B_f, C_f, 0, 0, 0)$ is the discretised affine state space representation of the sensor package, whilst $(\hat{A}_{sp}, \hat{B}_{sp}, [\hat{C}_{spe}, \hat{C}_{spt}], [\hat{D}_{spe}, \hat{D}_{spt}], \hat{e}_{sp}, \hat{f}_{sp})$ is the linearisation of (5) with respect to the short period states around the estimated disturbance states with the elevator and THS components separated, and $(A_a, B_a, C_a, 0, 0, 0)$ is the linear state space actuator model. Further augmented with the disturbance states,

Let: $\Delta\hat{C}_{M_{\alpha 2}} \leftarrow \max\{0, \Delta\hat{C}_{M_{\alpha 2}}\}$,
$\Delta\hat{C}_{L_{\alpha 2}} \leftarrow \min\{0, \Delta\hat{C}_{L_{\alpha 2}}\}$.
If $\hat{C}_{L_\alpha} + \hat{C}_{L_{\alpha 1}} < \hat{C}_{L_{\alpha,thresh}}$ **then**
$\hat{C}_{L_{\alpha 1}} \leftarrow \hat{C}_{L_{\alpha,thresh}} - \hat{C}_{L_\alpha}$ and $\Delta\hat{C}_{L_{\alpha 2}} \leftarrow 0$
elseif $\hat{C}_{L_\alpha} + \hat{C}_{L_{\alpha 1}} + \hat{C}_{L_{\alpha 2}}(\hat{\alpha} - \alpha_0) < \hat{C}_{L_{\alpha,thresh}}$
$\hat{C}_{L_{\alpha 2}} \leftarrow \max\{0, (\hat{C}_{L_{\alpha,thresh}} - \hat{C}_{L_{\alpha 1}} - \hat{C}_{L_\alpha})/(\hat{\alpha} - \alpha_0)\}$
endif

Algorithm 1. Parameter estimate thresholding

$$\begin{bmatrix} x_{aug}(k+1) \\ w(k+1) \end{bmatrix} = \begin{bmatrix} A_{aug} & B_w \\ 0 & A_w \end{bmatrix} \begin{bmatrix} x_{aug}(k) \\ w(k) \end{bmatrix} + \begin{bmatrix} B_{aug} & e_{tot} \\ 0 & 0 \end{bmatrix} \begin{bmatrix} u_t(k) \\ 1 \end{bmatrix}$$

$$y_{out} = \begin{bmatrix} C_{aug} & 0 \end{bmatrix} \begin{bmatrix} x_{aug}(k) \\ w(k) \end{bmatrix}$$

where $(A_w, B_w, e_{aug,w}, f_{aug,w})$ represent the linearisation of the model with respect to the disturbance states with their current values, and $e_{tot} = e_{aug} + e_{aug,w}$.

3. CONTROLLER DESIGN

Figure 3 depicts a high-level schematic of the integrated controller design. Measured flight data, along with estimated parameters are used to evaluate the surrogate model. This is used to compute a prestabilising gain, a constrained steady-state target and to update an Extended Kalman filter which estimates the plant and disturbance states, as well as to build matrices for a constrained MPC controller, which computes an additive perturbation to a nominal prestabilising control action.

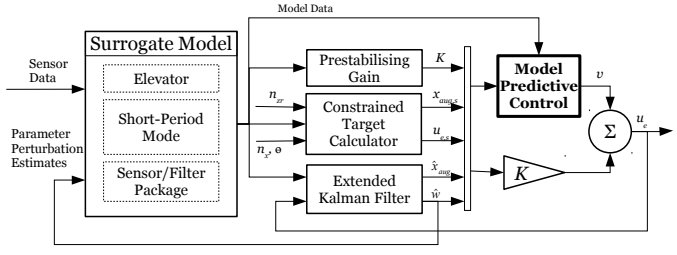

Fig. 3. High-Level Schematic of Integrated Design

3.1 Estimation: Extended Kalman Filter

The state estimation of the disturbance augmented model, $[\hat{x}_{aug}^T, \hat{w}^T]^T$, is performed using an Extended Kalman Filter (EKF) (e.g., Ljung (1979)). The process and measurement noise "covariance" matrices Q_k and R_k are chosen to be diagonal and tuned heuristically to achieve the desired performance. To avoid initial transients, we set the initial filter covariance matrix $P(0) = Q_k$ and iterate the Riccati equation 200 times on initialisation. We also hot-start the sensor, short-period and disturbance state estimates with values based on initial output measurements, the initial flight point and the initial THS position. Some simple thresholding is applied after the state vector estimate update stage of the EKF to ensure that the estimate of the total lift coefficient does not pass a stall threshold (which would lead to undesirable behaviour). For value $\hat{C}_{L_{\alpha,thresh}} > 0$ this is shown in Algorithm 1.

3.2 Constrained Target calculation

A constrained target calculator is used to compute a target setpoint pair $(x_{aug,s}, u_{e,s})$ solving a constrained quadratic program. Let C_α be a matrix selecting α from the state vector, and C_q be a matrix selecting q from the state vector, C_{n_z}, D_{n_z}, f_{n_z}, D_{wn_z} be matrices corresponding to the linearised output of the load factor from the state, input and modelled disturbance states, and $\hat{w}$ be the disturbance state estimate from the EKF. At each time step it computes

$$\min_{x_{aug,s}, u_{e,s}, \sigma} W\|\sigma\|_2^2 + \|(C_{n_z} x_{aug,s} + D_{n_z} u_{e,s} + f_{n_z} + D_{wn_z}\hat{w}) - n_{zr}\|_2^2$$

subject to

$$\begin{aligned} C_\alpha x_{aug,s} &\le \alpha_{\max} & -C_\alpha x_{aug,s} &\le -\alpha_{\min} \\ C_q x_{aug,s} &\le q_{\max} & -C_q x_{aug,s} &\le -q_{\min} \\ u_{e,s} &\le u_{\max} & -u_{e,s} &\le -u_{\min} \end{aligned}$$

$$\begin{aligned} (A_{aug} - I)x_{aug,s} + B_{aug}u_{e,s} + \sigma \\ = -B_w\hat{w} - e_{tot} - e_\alpha(2n_x g T_s)/(V_{\mathrm{TAS}} k_z \hat{C}_{L_\alpha}) \end{aligned}$$

where $W \gg 0$, n_{zr} is the reference command, σ is a vector of slack variables to ensure the optimisation is always feasible even if a compliant equilibrium does not exist, e_α is a vector with zeros on all elements apart from unity on the element corresponding to α, and n_x is the horizontal load factor, i.e., gravity normalised in-track acceleration. (This perturbs the "equilibrium" to account for the required value of α varying with speed and improves tracking when autothrust is disengaged. $n_x g T_s$ is the change in velocity in one time step. At equilibrium, $0.5\rho V_{\mathrm{TAS}}^2 C_L/(mg) \approx 1$. Assuming variation of C_L with V_{TAS} is small, $\partial n_z/\partial V_{\mathrm{TAS}} \approx 2/V_{\mathrm{TAS}}$. $\partial n_z/\partial\alpha = k_z\hat{C}_{L_\alpha}$. So, $-(\partial n_z/\partial V_{\mathrm{TAS}})/(\partial n_z/\partial\alpha) = -2/(V_{\mathrm{TAS}} k_z \hat{C}_{L\alpha})$ gives an approximation of how trim α_0 varies with V_{TAS}, which we use as an estimate of how the α required to hold any other load factor would vary.) The pitch rate limits are as follows:

$$\begin{aligned} q_{\max} &= \min\{q_{\max 0}, (\theta_{\max} - \theta)/\tau_\theta\} \\ q_{\min} &= \max\{q_{\min 0}, (\theta_{\min} - \theta)/\tau_\theta\} \end{aligned}$$

where θ is the pitch angle, $\theta_{\max} = 30°$, $\theta_{\min} = -15°$ are the pitch angle limits and $\tau_\theta = 3$ s is a tuning parameter for pitch angle protection. For the angle of attack we define:

$$\begin{aligned} \alpha_{\max} &= \min\{\alpha_{\max 0}, \alpha_{\max 0} + (2n_x g T_s)/(V_{\mathrm{TAS}} k_z \hat{C}_{L_\alpha})\tau_\alpha\} \\ \alpha_{\min} &= \alpha_{\min 0}. \end{aligned}$$

This "tightens" the constraint $\alpha_{\max 0}$ so that any commanded load factor would be safe if held for τ_α seconds assuming the current in-track acceleration. The variable $\alpha_{\max 0}$, varies with the flight condition, and comes from a lookup table as a function of airspeed and mach, whilst we take $\alpha_{\min 0}$ to be $-2°$. In principle, we could also employ the estimation of the variation of lift coefficient with respect to α to move the protection values, however in the simulation scenarios considered the nominal values appear already quite conservative and the behaviour of the pitching moment coefficient is more critical to determining the performance.

3.3 Pre-stabilising Inner Loop

Before MPC is applied, a time-varying, prestabilising unconstrained control gain is used. For homogeneous load factor transient responses over the flight envelope, we consider a virtual performance output vector y_z comprised

of the sensor outputs on q and n_z and their first derivatives (computed using the model). $[q_{sens}, n_{z,sens}, \dot{q}_{sens}, \dot{n}_{z\,sens}]$ and a time-varying control law manipulating $\Delta u_e(k) \triangleq u_e(k) - u_e(k-1)$, of the form

$$\Delta u_e(k) = K \begin{bmatrix} \hat{x}_{aug}(k) - x_{aug,s} \\ u_e(k-1) - u_{e,s} \end{bmatrix}$$

that minimises the cost function

$$J = \sum_{i=0}^{\infty} (y_z(i) - y_s)^T Q_y (y_z(i) - y_s) + \Delta u(i)^T R_y \Delta u(i)$$

based on the current local linear model, where y_s is the performance output corresponding to the setpoint pair. We approximate this by continuously iterating a Riccati difference equation. We choose $Q_y = \mathrm{diag}(0.2, 1, 0.1, 0.8)$, $R_y = 0.1$. This form allows damping of elevator transients and allows slew rate constraints in the next section.

3.4 Constrained MPC Control Law

Whilst the target calculation obtains a compliant setpoint, it does not provide transient constraint handling. For this, we implement a simple MPC control law based on perturbations to the predicted closed loop dynamics with hard constraints on elevator position and slew rate and soft constraints on outputs.

$$\tilde{A} \triangleq \begin{bmatrix} A_{aug} & B_{aug} & (e_{tot} + B_{dist}\hat{w}(k)) \\ 0 & 1 & 0 \\ 0 & 0 & 1 \end{bmatrix}, \quad \tilde{B} \triangleq \begin{bmatrix} B_{aug} \\ 1 \\ 0 \end{bmatrix},$$

$$\tilde{K} \triangleq \begin{bmatrix} K, & -K \begin{bmatrix} x_{aug,s}^T & u_{e,s}^T \end{bmatrix}^T \end{bmatrix}.$$

Let $(\tilde{C}_u, \tilde{D}_u)$, $(\tilde{C}_\alpha, \tilde{D}_\alpha)$ be matrices which selected the predicted elevator position and predicted α respectively from the augmented state, v_i be a predicted input increment perturbation i steps into the future, s_i be "slack variables", and W_{s1} and W_{s2} be positive weights. At each step, solve

$$\min_{\substack{v_i,\, i \in \{0,\ldots,N-1\} \\ s_i,\, i \in \{1,\ldots,N\}}} \sum_{i=0}^{N-1} \left(\|v_i\|^2 \right) + \sum_{i=1}^{N} \left(W_{s1}\|s_i\|_1 + W_{s2}\|s_i\|_2^2 \right)$$

subject to: $\tilde{x}_0 = [x_{aug}(k)^T, 1]^T$

$$\tilde{x}_{i+1} = (\tilde{A} + \tilde{B}\tilde{K})\tilde{x}_i + \tilde{B}v_i \quad i = \{0, \ldots, N-1\}$$

$$\Delta u_{\min} \le \tilde{K}\tilde{x}_i + v_i \le \Delta u_{\max}, \quad i = \{0, \ldots, N-1\}$$

$$u_{\min} \le \tilde{C}_u\tilde{x}_i + \tilde{D}_u v_i \le u_{\max}, \quad i = \{1, \ldots, N\}$$

$$-s_i + \alpha_{\min 0} \le \tilde{C}_\alpha\tilde{x}_i + \tilde{D}_\alpha v_i \le \alpha_{\max 0} + s_i, \quad i = \{1, \ldots, N\}.$$

This penalises deviations from the nominal unconstrained control law whilst satisfying slew rate and elevator position constraints, with a best-effort satisfaction of angle of attack constraints, with the penalty weighted by W_{s1} and W_{s2}. The 1-norm term is an "exact penalty", discouraging constraint violations if feasible. We choose horizon $N = 20$. The unconstrained control law is perturbed with v_0 and, following the receding horizon principle, the process repeated at each time step (Maciejowski, 2002).

4. SIMULATION RESULTS AND COMMENTS

The EKF, target calculator and predictive controller are all implemented in Simulink and Embedded MATLAB, with the latter two components employing a simple primal-dual interior point QP solver. This enables integration with the nonlinear RECONFIGURE benchmark. Figure 4 shows the closed loop simulation with a selection of flight conditions and load factor solicitations. Scenario (a) considers an aircraft towards the lighter end of the admissible range of mass with CoG towards the rear of the admissible range, at an altitude of 5000 ft and towards the lower end of the airspeed envelope. At $t = 5$ s, engine thrust is lowered to idle, and maximum load factor is solicited for 5 s. This is to test the angle of attack constraint. Scenario (b) considers a heavy aircraft with a forward CoG at the same altitude and airspeed. Trim engine trust is retained, and at $t = 5$ s, maximum load factor is solicited constantly. This also tests the angle of attack constraint. Scenario (c) considers the same configuration as secenario (b), but instead a sequence of steps is solicited. This tests load factor tracking performance at high incidence. Scenario (d) considers the same configuration as the scenario (a), except instead of lowering engine thrust, autothrust is engaged. This tests that the control law is robust to autothrust. For each of these scenarios, the simulation is performed firstly in a nominal scenario with a nominal tracking MPC control law emulated by setting the elements or Q_k in the EKF corresponding to the aerodynamic parameter estimates to zero. This gives qualitatively similar behaviour to the benchmark control law in the simulator, which the RECONFIGURE communication guidelines prohibit sharing. Then the same MPC control law is used with the maximum level of icing that the simulator permits. Finally the full EKF parameter-estimation based MPC control law is demonstrated. With the nominal MPC, the scenarios with icing all exhibit large magnitude oscillations and the upper limit on α is violated. With the EKF-based MPC, the trajectories are substantially better damped and more comparable with the nominal situation. Moreover, the limit on α is not violated.

5. CONCLUSIONS

This paper has shown the effectiveness of linear time-varying MPC with aerodynamic parameter estimation using an EKF to improve the performance of the inner loop control and angle of attack protection of the RECONFIGURE benchmark in scenarios where ice accretion causes substantial changes in aerodynamic behaviour. Damping of transients is improved, and adherence to angle of attack limits is also improved. Future work will involve consideration of different observer designs, such as moving horizon estimation (MHE) to further improve performance and robustness, and application of more efficient computational implementations of the MPC component, as well as consideration of appropriate integration and clearance approaches.

REFERENCES

Bragg, M.B., Basar, T., Perkins, W.R., Seig, M.S., Voulgaris, P.G., Melody, J.W., and Sarter, N.B. (2002). Smart icing systems for aircraft icing safety. In *40th AIAA Aerospace Sciences Meeting and Exhibit*. Reno, NV.

Brière, D., Favre, C., and Traverse, P. (1995). A family of fault-tolerant systems: electrical flight controls, from Airbus A320/330/340 to future military transport aircraft. *Microprocessors and Microsystems*, 19(2), 75–82.

Cao, Y., Wu, Z., Su, Y., and Xu, Z. (2015). Aircraft flight characteristics in icing conditions. *Prog. Aerospace Sci.*, 74(0), 62–80.

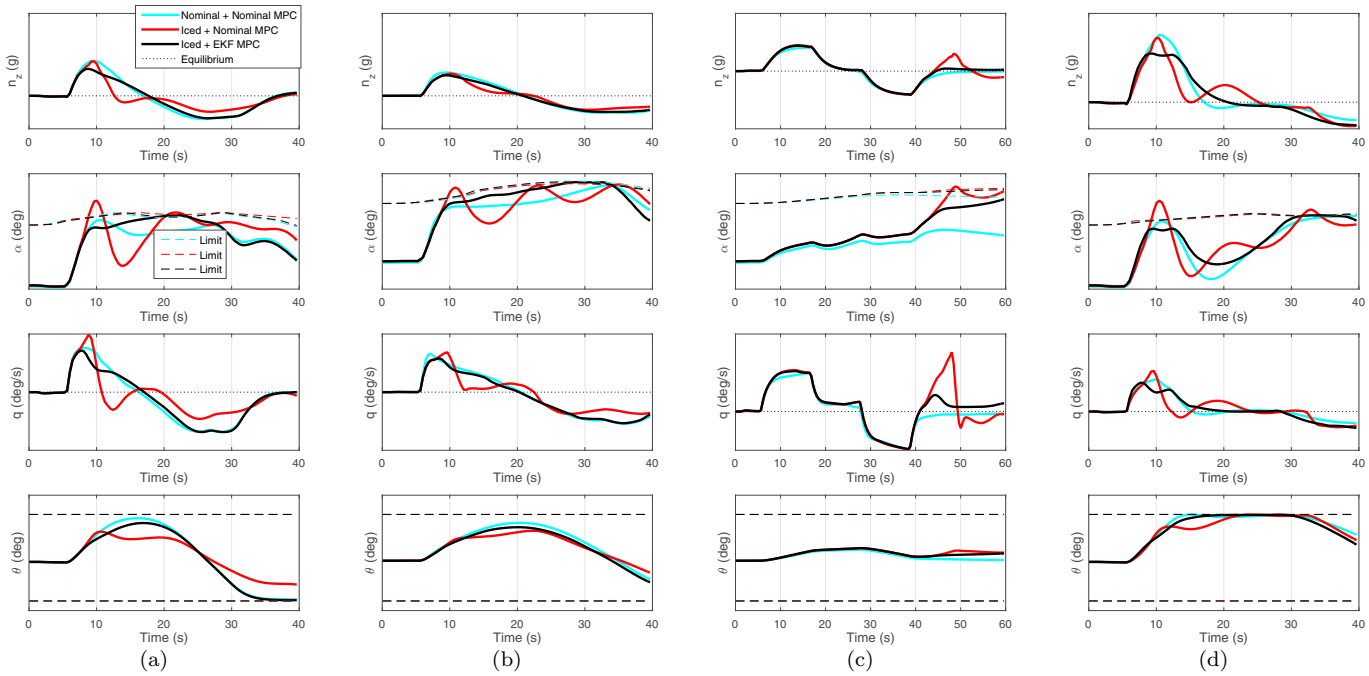

Fig. 4. Closed-loop trajectories comparing nominal MPC with EKF-based MPC in icing scenarios

Cebeci, T. and Kafyeke, F. (2003). Aircraft icing. *Annual Review of Fluid Mechanics*, 35, 11–21.

Falkena, W., Borst, C., Chu, Q.P., and Mulder, J.A. (2011). Investigation of practical flight envelope protection systems for small aircraft. *J. Guidance, Control, and Dynamics*, 34(4), 976–988.

Favre, C. (1994). Fly-by-wire for commercial aircraft: the Airbus experience. *Int. J. Control*, 59(1), 139–157.

Goupil, P., Boada-Bauxell, J., Marcos, A., Cortet, E., Kerr, M., and Costa, H. (2014). AIRBUS efforts towards advanced real-time fault diagnosis and fault tolerant control. In *Proc. 19th IFAC World Congress*, 3471–3476. Cape Town, South Africa.

Gros, S., Quirynen, R., and Diehl, M. (2012). Aircraft control based on fast non-linear MPC & multiple-shooting. In *Proc. 51st IEEE Conf. on Decision and Control*, 1142–1147. Maui, HI, USA.

Hossain, K., Sharma, V., Bragg, M., and Voulgaris, P. (2003). Envelope protection and control adaptation in icing encounters. In *41st Aerospace Sciences Meeting and Exhibit*. Reno, Nevada.

Kale, M.M. and Chipperfield, A.J. (2004). Robust and stabilized MPC formulations for fault tolerant and reconfigurable flight control. In *Proc. IEEE Int. Symp. Intelligent Control*, 222–227. Taipei, Taiwan.

Keviczky, T. and Balas, G.J. (2006). Software-enabled receding horizon control for autonomous unmanned aerial vehicle guidance. *J. Guidance, Control, and Dynamics*, 29(3), 680–694.

Ljung, L. (1979). Asymptotic behavior of the extended Kalman filter as a parameter estimator for linear systems. *IEEE Trans. Automat. Control*, 24(1), 36–50.

Lombaerts, T., Huisman, H., Chu, P., Mulder, J.A., and Joosten, D. (2009). Nonlinear reconfiguring flight control based on online physical model identification. *J. Guidance, Control, and Dynamics*, 32(3), 727–748.

Lynch, F.T. and Khodadoust, A. (2001). Effects of ice accretions on aircraft aerodynamics. *Prog. Aerospace Sci.*, 37(8), 669–767.

Maciejowski, J.M. (2002). *Predictive Control with Constraints*. Pearson Education.

Maeder, U., Borrelli, F., and Morari, M. (2009). Linear offset-free model predictive control. *Automatica*, 45(10), 2214–2222.

Melody, J.W., Başar, T., Perkins, W.R., and Voulgaris, P.G. (2000). Parameter identification for inflight detection and characterization of aircraft icing. *Control Eng. Pract.*, 8(9), 985–1001.

Muske, K.R. and Badgwell, T.A. (2002). Disturbance modeling for offset-free linear model predictive control. *J. Process Control*, 12(5), 617–632.

Pannocchia, G. and Rawlings, J.B. (2003). Disturbance models for offset-free model predictive control. *AIChE J.*, 49(2), 426–437.

Sharma, V., Voulgaris, P.G., and Frazzoli, E. (2004). Aircraft autopilot analysis and envelope protection for operation under icing conditions. *J. Guidance, Control, and Dynamics*, 27(3), 454–465.

Tang, L., Roemer, M., Ge, J., Crassidis, A., Prasad, J., and Belcastro, C. (2009). Methodologies for adaptive flight envelope estimation and protection. In *AIAA Guidance, Navigation, and Control Conf.*

Vinnicombe, G. (1999). A ν-gap distance for uncertain and nonlinear systems. In *Proc. 38th IEEE Conf. Decision and Control*, 2557–2562. Phoenix, AZ.

Well, K.H. (2006). Aircraft control laws for envelope protection. In *AIAA Guidance, Navigation, and Control Conf. and Exhibit*. Keystone, CO.

Yu, M.J., McDonough, K., Bernstein, D.S., and Kolmanovsky, I. (2014). Retrospective cost model refinement for aircraft fault signature detection. In *Proc. American Control Conf.*, 2486–2491. Portland, OR.